



HOKKAIDO UNIVERSITY

Title	Satellite X-Ray Scattering and Structural Modulation of Thiourea
Author(s)	塩崎, 洋一; Shiozaki, Yoichi
Degree Grantor	北海道大学
Degree Name	博士(理学)
Dissertation Number	乙第853号
Issue Date	1971-03-25
Doc URL	https://hdl.handle.net/2115/91059
Type	doctoral thesis
File Information	Yoichi_Shiozaki.pdf,



Satellite X-Ray Scattering and Structural
Modulation of Thiourea

Yôichi Shiozaki

Department of Physics, Faculty of Science,
Hokkaido University, Sapporo, Japan.

Synopsis

Integrated intensities have been measured of the satellite x-ray scatterings which appear in the intermediate phases II, III and IV of thiourea. The structural modulation which causes the satellite scattering is assumed to be a sinusoidal transverse wave of atomic shifts with the wave number vector parallel to the c axis. Parameters which characterize

the modulation at -86°C are determined by a least squares calculation, and agreement is obtained between the observed and calculated scattering amplitudes with the discrepancy factor R of 0.16. Intensities of several Bragg and satellite scatterings have been measured as functions of temperature by a single crystal diffractometer and expression on the temperature dependence of the modulation parameters are deduced.

§1 Introduction

Ferroelectricity in thiourea was discovered by Solomon in 1956.¹⁾ This crystal has five phases between the liquid nitrogen and the room temperatures.²⁾ The transition temperatures are -104°C , -97°C , -94°C and -71°C . These phases are named as I, II, III, IV and V from low temperature phase, respectively. Figure 1 shows dielectric constant as a function of temperature and the five phases after Goldsmith and White.²⁾ The phase I is ferroelectric whose polarization is parallel to the b axis* and the phase V is generally called paraelectric. The phase III in the intermediate

*There are two ways to assign the crystallographic axes a , b , c in thiourea: one was adopted by Goldsmith and White²⁾ and the other by Kunchur and Truter.³⁾ In the present paper the system of Goldsmith and White is used.

temperature range is also ferroelectric whose spontaneous polarization is as small as 10^{-3} times of that in the phase I. Several workers made structure analyses of the phases I and V by means of x-ray and neutron diffraction.^{2,3,4,5)} According to their analyses, unit cell contains four molecular units. The space groups of the phases I and V are $Pb2_1m$ and $Pbnm$, respectively. A model was proposed to explain the dielectric anomalies by Calvo.⁶⁾ In 1962, Futama made hysteresis and thermal studies of all the phases,⁷⁾ and in 1963, Futama and Chiba first observed satellite x-ray scatterings in the phase IV.⁸⁾ Further investigations showed that the satellite scatterings are present not only in the phase IV but also in the phases II and III, and their intensities varied continuously and smoothly within the experimental error through the phases II, III and IV.^{9,10)} The satellite x-ray scattering suggests that there exists a structural modulation in the intermediate phases II, III and IV. The purpose of this study was to find out the nature of this structural modulation.

A preliminary report on our work was published in 1970.¹¹⁾ Somewhat similar structural works were made in other laboratories and brief reports have been published by Tanisaki and Nakamura¹²⁾ and by Futama.¹³⁾ Discussion will be made in connection with their results in §7.

§2 Experimental Procedures

Cylindrical specimens parallel to the a and c axes, respectively were prepared. The lengths of the specimens were about 1 mm and the diameters were less than 0.3 mm. The specimen was cooled by a gas blow method of nitrogen from a liquid nitrogen vessel with heater. $\text{CuK}\alpha$ radiation was used in all experiments. Weissenberg photographs of $(h0l)$ and $(0kl)$ reciprocal planes were taken to survey general features of the intensity distribution of the scattered x-rays at -100°C in the phase II, at -95°C in the phase III, at -86°C in the phase IV and at several other temperatures, where (hkl) is the Miller indices. Also photographs of $(1kl)$ and $(2kl)$ were taken around -95°C . A scintillation counter and a LiF crystal monochromator were used to investigate temperature dependence of the scattered x-rays.

§3 General Features of Satellite Scatterings

The Weissenberg photographs proved that the general features of the distribution of diffracted intensities are common in the phases II, III and IV. An example of the Weissenberg photographs is shown in Fig. 2.

Below discussion will be made on the intensity

distribution by referring to the "unperturbed structure" imagined in the phases II, III and IV. It is similar to the structure of the room temperature phase V in the sense that its space group is Pbnm and its unit cell vectors \underline{a} , \underline{b} , \underline{c} are almost the same as those in the phase V. ($a=5.52\text{\AA}$, $b=7.66\text{\AA}$, $c=8.54\text{\AA}$ at 20°C in the phase V.⁵⁾) The unperturbed structure will be realized if the structural modulation described below were put equal to zero. The reciprocal lattice vectors of this unperturbed structure are denoted as \underline{a}^* , \underline{b}^* , \underline{c}^* . The Miller indices (hkl) will be referred to the above-defined \underline{a} , \underline{b} , \underline{c} . Distribution of the scattered x-rays on the $\underline{b}^*-\underline{c}^*$ and $\underline{a}^*-\underline{c}^*$ planes are depicted schematically in Fig. 3. The satellite scatterings take place at $(h, k, l \pm n\delta)$ in the reciprocal space as seen in Fig. 3 and as was observed on the photographs of $(1kl)$ and $(2kl)$ reciprocal planes. Here n is an integer and δ is the distance in fraction between the main and the first satellite scattering in reciprocal space, where the main scattering means the Bragg reflection at (hkl) and the first satellite means the one nearest to the main spot. The maximum value of n observed so far was 3. Values of δ were determined at various temperatures by measuring the diffraction angles of the (020) and (02δ) reflections with a single crystal diffractometer. Figure 4 shows $1/\delta$ as a function of temperature.

As described in §1, the space group is Pbnm in the phase V and $Pb2_1m$ in the phase I, that is, the b-glide symmetry exists in both phases but the n-glide symmetry is destroyed by the occurrence of the spontaneous polarization. The distribution of the satellite spots demonstrated in Fig. 3(a) proves that there exists the b-glide also in the phases II, III and IV because diffraction spots appear only at $(0, k, l \pm n\delta)$ with $k = \text{even}$. It is interesting to observe in Fig. 3(b) that no Bragg spots appear at $(h0l)$ with $h+l = \text{odd}$ but satellite spots appear around these points and also that no satellite spots are observed around $(h0l)$ with $h+l = \text{even}$. These features, which may be called a pseudo-extinction rule, can be explained by assuming that the unperturbed structure has the space group Pbnm but the n-glide is destroyed by the structural modulation, as discussed in §4. Theoretically,^{14,15)} the fact that the satellites appear only at $(h, k, l \pm n\delta)$ implies that the crystal structure is modulated by a sinusoidal wave with wave number vector δc^* and in general by additional harmonic waves. Korekawa presented, in his review article,¹⁶⁾ typical patterns of satellite scatterings caused by the modulation of atomic scattering amplitude and those caused by the longitudinal and transverse wave modulations of atomic positions, when the modulation is expressed by a pure sine wave. Characteristic features of the results of

these three types of modulations are as follows, when the wave number vector of modulation is δ_c^* . The satellite scatterings appear only at $(h, k, l \pm \delta)$ in case of the amplitude modulation. In cases of the modulation of atomic positions, satellites appear generally at $(h, k, l \pm n\delta)$. Intensities of the satellites increase with increasing l in case of the modulation of atomic positions by the longitudinal wave, and increase with k in case of the modulation of atomic shifts by the transverse wave, when the polarization of the transverse wave is parallel to the b axis. The general features of the satellites observed in thiourea is in agreement with the case of the transverse wave modulation, as seen in Fig. 3(a). Especially, if the modulation wave has a longitudinal character, satellite spots should be expected around $(00l)$. However, no satellite was observed at $(0, 0, l \pm n\delta)$. Therefore, the modulation is assumed to be a pure transverse wave in the following discussion.

§4 Models and Formulation

On the basis of the experimental observations described above, the following postulations are made to explain the satellite x-ray scattering.

- (1) For simplicity, the structural modulations of the

Throughout the following discussions we put $z=1/4$ for S and C atoms so that eight $(SC)_{1/2}NH_2$ molecules are identical to four $SC(NH_2)_2$.

Figure 6 shows the unit cell when the structural modulation is introduced. The numbered circle in Fig. 6 stands for any atom of the thiourea molecule having the same number in Fig. 5. The arrows show x and y components of atomic displacements as a result of the modulation. (They are drawn referring to Eqs. (17) and (19) discussed later.) The b-glide symmetry still exists as assumed above and the positions of the atoms 2 and 4 can be expressed by the positions 1 and 3, respectively. Therefore, the crystal may be decomposed into two sublattices: sublattice 1 consists of molecules 1 and 2, and sublattice 2 of molecules 3 and 4. The longitudinal displacements of atoms do not occur as assumed at the beginning of this section, and therefore, the z-parameters of all atoms are not changed by the modulation. Below each atom in thiourea molecule will be numbered and expressed as the j-th atom ($j=1$ corresponds to S, etc.). Its position in the unperturbed structure will be denoted by x_j , y_j and z_j . The unit cell of which origin is at $n_1\underline{a}+n_2\underline{b}+n_3\underline{c}$ will be called the n-th unit cell. Now the modulation on the x-parameters of the j-th atom Δx_j in the sublattice 1 of the n-th unit cell will be expressed as

$$\Delta x_j = \alpha_{j1} \sin 2\pi \left(\frac{n_3}{M} + \varphi_{xj1} \right) \quad (1)$$

Here α_{j1} is amplitude, M is the wave length and φ_{xj1} is the phase parameter. The parameter M will be called a period and related to δ by

$$M = 1/\delta. \quad (2)$$

Temperature dependence of M was already shown in Fig. 4.

The symbol α_{j1} will be replaced by β_{j1} for the y -parameter, and the suffix 1 will be changed to 2 for the sublattice 2.

As a result of the structural modulation, the eight positions listed above are now as follows.

$$\left. \begin{aligned} & (x_j + \alpha_{j1} \sin 2\pi \left(\frac{n_3}{M} + \varphi_{xj1} \right), y_j + \beta_{j1} \sin 2\pi \left(\frac{n_3}{M} + \varphi_{yj1} \right), z_j), \\ & (x_j + \alpha_{j1} \sin 2\pi \left(\frac{n_3}{M} + \varphi_{xj1} \right), y_j + \beta_{j1} \sin 2\pi \left(\frac{n_3}{M} + \varphi_{yj1} \right), \frac{1}{2} - z_j), \\ & (\frac{1}{2} - x_j + \alpha_{j1} \sin 2\pi \left(\frac{n_3}{M} + \frac{1}{2} + \varphi_{xj1} \right), \frac{1}{2} + y_j + \beta_{j1} \sin 2\pi \left(\frac{n_3}{M} + \varphi_{yj1} \right), z_j), \\ & (\frac{1}{2} - x_j + \alpha_{j1} \sin 2\pi \left(\frac{n_3}{M} + \frac{1}{2} + \varphi_{xj1} \right), \frac{1}{2} + y_j + \beta_{j1} \sin 2\pi \left(\frac{n_3}{M} + \varphi_{yj1} \right), \frac{1}{2} - z_j), \\ & (\frac{1}{2} + x_j + \alpha_{j2} \sin 2\pi \left(\frac{n_3}{M} + \frac{1}{2} + \varphi_{xj2} \right), \frac{1}{2} - y_j + \beta_{j2} \sin 2\pi \left(\frac{n_3}{M} + \varphi_{yj2} \right), \frac{1}{2} + z_j), \\ & (\frac{1}{2} + x_j + \alpha_{j2} \sin 2\pi \left(\frac{n_3}{M} + \frac{1}{2} + \varphi_{xj2} \right), \frac{1}{2} - y_j + \beta_{j2} \sin 2\pi \left(\frac{n_3}{M} + \varphi_{yj2} \right), 1 - z_j), \\ & (1 - x_j + \alpha_{j2} \sin 2\pi \left(\frac{n_3}{M} + \varphi_{xj2} \right), 1 - y_j + \beta_{j2} \sin 2\pi \left(\frac{n_3}{M} + \varphi_{yj2} \right), \frac{1}{2} + z_j), \\ & (1 - x_j + \alpha_{j2} \sin 2\pi \left(\frac{n_3}{M} + \varphi_{xj2} \right), 1 - y_j + \beta_{j2} \sin 2\pi \left(\frac{n_3}{M} + \varphi_{yj2} \right), 1 - z_j). \end{aligned} \right\} (3)$$

The former four positions belong to the sublattice 1 and the latter four to the sublattice 2. Denoting the atomic scattering factor of the j -th atom as f_j ,

the structure amplitude of the sublattice 1 of the n-th unit cell $F_{1,n}$ is given by

$$\begin{aligned}
 F_{1,n} = & \sum_j f_j \\
 & \times \left[e^{i2\pi(\xi\{x_j + \alpha_{j1}\} \sin 2\pi(\frac{n_3}{M} + \varphi_{xj1}) + \eta\{y_j + \beta_{j1}\} \sin 2\pi(\frac{n_3}{M} + \varphi_{yj1}) + \zeta z_j)} \right. \\
 & + e^{i2\pi(\xi\{x_j + \alpha_{j1}\} \sin 2\pi(\frac{n_3}{M} + \varphi_{xj1}) + \eta\{y_j + \beta_{j1}\} \sin 2\pi(\frac{n_3}{M} + \varphi_{yj1}) + \zeta\{\frac{1}{2} - z_j\})} \\
 & + e^{i2\pi(\xi\{\frac{1}{2} - x_j + \alpha_{j1}\} \sin 2\pi(\frac{n_3}{M} + \frac{1}{2} + \varphi_{xj1}) + \eta\{\frac{1}{2} + y_j + \beta_{j1}\} \sin 2\pi(\frac{n_3}{M} + \varphi_{yj1}) + \zeta z_j)} \\
 & \left. + e^{i2\pi(\xi\{\frac{1}{2} - x_j + \alpha_{j1}\} \sin 2\pi(\frac{n_3}{M} + \frac{1}{2} + \varphi_{xj1}) + \eta\{\frac{1}{2} + y_j + \beta_{j1}\} \sin 2\pi(\frac{n_3}{M} + \varphi_{yj1}) + \zeta\{\frac{1}{2} - z_j\})} \right], \quad (4)
 \end{aligned}$$

where ξ , η and ζ are components of a position vector in reciprocal space. The total structure amplitude F_1 of the sublattice 1 of whole the crystal bathed in the incident x-rays is given by summing $F_{1,n}$ with respect to n_1 , n_2 and n_3 :

$$F_1 = \sum_{n_1} \sum_{n_2} \sum_{n_3} F_{1,n} e^{i2\pi(\xi n_1 + \eta n_2 + \zeta n_3)} \quad (5)$$

By using the relation $\exp(i\alpha \sin \theta) = \sum_{n=-\infty}^{\infty} J_n(\alpha) \exp(in\theta)$, where J_n is the Bessel function of the n-th order, we have

$$\begin{aligned}
 F_1 = & G(\hbar) G(k) \sum_j 2f_j e^{i2\pi\frac{\zeta}{4} \cos 2\pi\zeta(z_j - \frac{1}{4})} \\
 & \times \left[e^{i2\pi(\hbar x_j + k y_j)} \sum_{n=-\infty}^{\infty} \sum_{m=-\infty}^{\infty} J_n(2\pi\hbar\alpha_{j1}) J_m(2\pi k\beta_{j1}) \right. \\
 & \times e^{i2\pi(n\varphi_{xj1} + m\varphi_{yj1})} G\left(\zeta + \frac{n+m}{M}\right) \\
 & + e^{i2\pi(\hbar(\frac{1}{2} - x_j) + k(\frac{1}{2} + y_j))} \sum_{n=-\infty}^{\infty} \sum_{m=-\infty}^{\infty} J_n(2\pi\hbar\alpha_{j1}) J_m(2\pi k\beta_{j1}) \\
 & \left. \times e^{i2\pi(\frac{n}{2} + n\varphi_{xj1} + m\varphi_{yj1})} G\left(\zeta + \frac{n+m}{M}\right) \right]. \quad (6)
 \end{aligned}$$

Here G is related to the Laue interference function L by $|G|^2 = L$. The functions $G(\xi)$ and $G(\eta)$ directly resulted from Eq. (5) are written as $G(h)$ and $G(k)$ in Eq. (6), where h and k are integers. The Laue function $|G(\xi + \frac{n+m}{M})|^2$ has the finite value only for $\xi + \frac{n+m}{M} = l$ (integers), and thus gives the main and satellite scatterings at $\xi = l - \frac{n+m}{M}$. In the same way as above, we have the structure amplitude F_2 of the sublattice 2 as

$$\begin{aligned}
 F_2 = & G(h)G(k) \sum_j 2f_j e^{i2\pi \frac{3}{4} \xi} \cos 2\pi \xi (z_j - \frac{1}{4}) \\
 & \times \left[e^{i2\pi (h(\frac{1}{2} + x_j) + k(\frac{1}{2} - y_j))} \sum_n \sum_m J_n(2\pi h \alpha_{j2}) J_m(2\pi k \beta_{j2}) \right. \\
 & \times e^{i2\pi (\frac{n}{2} + n \varphi_{xj2} + m \varphi_{yj2})} G(\xi + \frac{n+m}{M}) \\
 & + e^{i2\pi (h(1-x_j) + k(1-y_j))} \sum_n \sum_m J_n(2\pi h \alpha_{j2}) J_m(2\pi k \beta_{j2}) \\
 & \left. \times e^{i2\pi (n \varphi_{xj2} + m \varphi_{yj2})} G(\xi + \frac{n+m}{M}) \right]. \quad (7)
 \end{aligned}$$

The total structure amplitude F of the structurally modulated crystal is given by adding F_1 and F_2 :

$$F = F_1 + F_2 \quad (8)$$

The expression (8) becomes easy to handle in the case of either $k=0$ or $h=0$. The modulation parameters will be determined by using these reflections in the next section and the structure amplitudes are treated in more detail in these cases below.

The Scattering Amplitude for $(h, 0, l \pm n\delta)$

Simple calculations lead us to the following expression

of the structure amplitude for the main and satellite scatterings at $(h, 0, l - n\delta)$.

$$\begin{aligned}
 F &= 2G(\hbar) G(\hbar) \sum_j f_j e^{i2\pi \frac{\hbar+\xi}{4} z_j} \cos 2\pi \xi (z_j - \frac{1}{4}) \\
 &\times \sum_n \left[\left\{ e^{i2\pi \hbar (x_j - \frac{1}{4})} + e^{i2\pi \frac{n}{2}} e^{i2\pi \hbar (\frac{1}{4} - x_j)} \right\} \right. \\
 &\times \left\{ J_n(2\pi \hbar \alpha_{j1}) e^{i2\pi n \varphi_{xj1}} + e^{i2\pi \frac{\hbar+\xi-n}{2}} J_n(2\pi \hbar \alpha_{j2}) e^{i2\pi n \varphi_{xj2}} \right\} \\
 &\left. \times G\left(\xi + \frac{n}{M}\right) \right] \quad (9)
 \end{aligned}$$

In this equation n can be either positive or negative.

As mentioned in §3, there are characteristic features in the intensity distribution on the $(h0l)$ reciprocal plane, that is, the Bragg spots appear only for $h+l=\text{even}$, while the satellites $(h, 0, l \pm \delta)$ are present only for $h+l=\text{odd}$. This pseudo-extinction rule can be explained by examining the factor in Eq.(9):

$$\begin{aligned}
 B &\equiv J_n(2\pi \hbar \alpha_{j1}) e^{i2\pi n \varphi_{xj1}} \\
 &+ e^{i2\pi \frac{\hbar+\xi-n}{2}} J_n(2\pi \hbar \alpha_{j2}) e^{i2\pi n \varphi_{xj2}} \quad (10)
 \end{aligned}$$

If we neglect terms higher than the second power in the Taylor series expansion of the Bessel function $J_n(x)$, we have $J_0(x)=1$, $J_1(x)=x/2$ and $J_n(x)=0$ for $n \geq 2$. By this approximation, we have the following relations. In case of $n=0$ (main scattering),

$$B = 2 \quad (11)$$

for $h+l=\text{even}$, and

$$B = 0 \quad (12)$$

for $h+l=\text{odd}$. In case of $n=1$ (the first satellites),

$$B = \pi \hbar e^{i2\pi \varphi_{xj1}} [\alpha_{j1} - \alpha_{j2} e^{-i2\pi \frac{1}{2M}} e^{i2\pi(\varphi_{xj2} - \varphi_{xj1})}] \quad (13)$$

for $h+l=\text{even}$, and

$$B = \pi \hbar e^{i2\pi \varphi_{xj1}} [\alpha_{j1} + \alpha_{j2} e^{-i2\pi \frac{1}{2M}} e^{i2\pi(\varphi_{xj2} - \varphi_{xj1})}] \quad (14)$$

for $h+l=\text{odd}$. In case of $n \geq 2$,

$$B = 0. \quad (15)$$

Here α_{j1} and α_{j2} are defined as amplitude, the positive real quantity, and therefore, the pseudo-extinction rule are explained by putting

$$\left. \begin{aligned} \varphi_{xj2} &= \varphi_{xj1} + \frac{1}{2M} \\ \alpha_{j1} &= \alpha_{j2} \end{aligned} \right\} \quad (16)$$

Since $M \cong 10$, these relations are approximately equivalent to

$$\left. \begin{aligned} \alpha_{j1} &= \alpha_{j2} \\ \varphi_{xj1} &= \varphi_{xj2} \end{aligned} \right\} \quad (17)$$

The relations (17) will be assumed to hold exactly throughout the calculation described below, in order to make the calculation simple. The arrows parallel or antiparallel to the a axis in Fig. 6 were drawn by taking into account of Eqs. (17).

The Scattering Amplitude for $(0, k, l \pm n\delta)$

As in the case for $(h, 0, l \pm n\delta)$, we get the following

expression of the structure amplitude for the main and satellite scatterings at $(0, k, l-n\delta)$.

$$\begin{aligned}
 F = & 4G(h)G(k)e^{i2\pi\frac{\xi}{4}} \cos 2\pi\frac{k}{4} \sum_j f_j \cos 2\pi\xi(z_j - \frac{1}{4}) \\
 & \times \sum_n \left[\left\{ e^{i2\pi k(\frac{1}{4} + y_j)} J_n(2\pi k \beta_{j1}) e^{i2\pi n y_{j1}} \right. \right. \\
 & \left. \left. + e^{i2\pi\frac{\xi}{2}} e^{i2\pi k(\frac{3}{4} - y_j)} J_n(2\pi k \beta_{j2}) e^{i2\pi n y_{j2}} \right\} \right. \\
 & \left. \times G\left(\xi + \frac{n}{M}\right) \right] \quad (18)
 \end{aligned}$$

In this equation n can be either positive or negative. As described in §3, there is the extinction rule characteristic to the b-glide: diffraction spots are present only at $(0, k, l-n\delta)$ with k =even. The factor $\cos(2\pi k/4)$ in Eq. (18) is resulted from the presence of the b-glide and explains the extinction rule.

§5 Atomic Positions in the Structurally Modulated Crystal at -86°C

In this section, atomic positions in the structurally modulated crystal are determined by means of least squares calculation, based on Eqs. (9) and (18).

For the calculation the following assumptions are made.

(1) The parameters z_j are constant, since the modulation wave is pure transverse as assumed in §4. Values of

z_j are assumed to be the same as those in the phase V,⁵⁾ which are shown in Table I.

(2) For simplicity, anisotropic temperature factors assigned to each atom are determined by interpolation of the values in the phases I and V.⁵⁾ The values adopted in our calculation are shown in Table I.

(3) The relations (17) are assumed.

(4) The following relations are assumed.

$$\left. \begin{aligned} \beta_{j1} &= \beta_{j2} \\ \varphi_{yj1} &= \varphi_{yj2} \end{aligned} \right\} \quad (19)$$

In Fig. 6, the arrows which express the y components of the atomic shifts have been drawn taking into account these relations. It was observed that the satellites at $(0, k, l \pm n\delta)$ with $l = \text{odd}$ were weak and those with $l = \text{even}$ were strong in general. Preliminary calculations were made by assuming the counter-phase modulation of the sublattices 1 and 2, i.e., by putting $\varphi_{yj1} = \varphi_{yj2} + 0.5$, without success in interpreting the above-described features of $(0, k, l \pm n\delta)$ scatterings. Therefore, $\varphi_{yj1} = \varphi_{yj2}$ is a better assumption than putting $\varphi_{yj1} = \varphi_{yj2} + 0.5$. The relations of Eq. (19) are, however, an assumption which we were forced to put due to the limitation of the memory capacity of our computer FACOM 270-20. We hope refine this point when more precise data will be collected. On the basis of Eqs. (17) and (19), the notations $\alpha_j, \beta_j, \varphi_{xj}, \varphi_{yj}$ will be used for α_{j1} .

and α_{j2} , β_{j1} and β_{j2} , φ_{xj1} and φ_{xj2} , φ_{yj1} and φ_{yj2} , respectively.

(5) It is assumed that φ_{xj} and φ_{yj} can have only the values of either 0 or 0.5. This will happen if the thiourea molecule is rigid and if the modulation corresponds to pure rotation or pure translation of the molecule or to combination of them in phase or in antiphase.

(6) Contribution of the hydrogen atoms to the x-ray scattering was neglected in the calculation, since the data did not seem to be so good.

(7) The period M of the modulation wave which appears in Eqs. (9) and (18) are put equal to 8.4 at -86°C . This value was determined by the observation shown in Fig. 4, where $M=1/\delta$.

On these assumptions the variable parameters to be refined by the least squares calculation are x_j , y_j , α_j and β_j with $j = \text{S, C, N}$, as seen in the expression (3). The least squares calculations were made for all possible combinations of the values (0 or 0.5) of φ_{xj} and φ_{yj} . As described below two combinations resulted in good agreement with the observation. The choice of one from the two was made by the criterion that the thiourea molecule does not deform drastically by the modulation.

The intensity data were collected from the Weissenberg photographs taken at -86°C . The data on $(h, 0, l - \delta)$ and $(0, k, l - n\delta)$ with $n=1, 2$ were used to determine x_j and

α_j by Eq. (9) and y_j and β_j by Eq. (18), respectively.

The least squares calculation was made so as to minimize $R \equiv \sum (|F_o| - |F_c|)^2$, where F_o and F_c are the observed and the calculated structure factors, respectively. The derivatives of J_n were expressed by J_{n-1} and J_{n+1} and, as mentioned in §4, the four $SC(NH_2)_2$ molecules in unit cell were treated as eight $(SC)_{1/2}NH_2$ molecules in the programming. The trial values of x_j and y_j used at the first cycle of the least squares calculation were those in the room temperature structure (phase V). Primitive calculations suggested that the orders of magnitudes of α_j and β_j are 0.02, which were used as the trial values of them in the first cycle of the calculation. For each combination of the values (0 or 0.5) of φ_{xj} and φ_{yj} , three or four cycles of least squares calculation gave steady values of R , where $R \equiv \sum ||F_o| - |F_c|| / \sum |F_c|$. The six parameters x_j and α_j were determined by using Eq. (9) and 110 integrated intensities of $(h, 0, l)$ and $(h, 0, l - \delta)$ reflections as listed in Table III(a). The least squares calculations were made for all the combinations of the values (0 and 0.5) of φ_{xj} , except for the combinations which resulted in bending of the thiourea molecule. The lowest value (0.16) of R was obtained for the same values of φ_{xS} , φ_{xC} and φ_{xN} (i.e., for the case of in-phase) and for the values of x_j and α_j listed in Table II. The six parameters y_j and β_j were determined

by using Eq. (18) and 111 integrated intensities of $(0, k, l)$, $(0, k, l - \delta)$ and $(0, k, l - 2\delta)$ reflections, which are shown in Table III(b). The minimum value (0.16) of R was obtained for the values of y_j and β_j listed in Table II, when φ_{yN} differs by 0.5 from φ_{yS} and φ_{yC} . As far as the agreement between $|F_o|$ and $|F_c|$ is concerned, the same result is obtained for the following four combinations of $(\varphi_{xS}, \varphi_{xC}, \varphi_{xN}, \varphi_{yS}, \varphi_{yC}, \varphi_{yN})$:
 $C_1 = (0.5, 0.5, 0.5, 0, 0, 0.5)$, $C_2 = (0, 0, 0, 0.5, 0.5, 0)$,
 $C_3 = (0, 0, 0, 0, 0, 0.5)$, $C_4 = (0.5, 0.5, 0.5, 0.5, 0.5, 0)$.
 Physically, the combination C_1 is identical to C_2 and C_3 is identical to C_4 . The difference between C_1 and C_3 can be seen by the fact that C_1 gives negative y component of displacement to the S atom when its x component is positive, while C_3 gives positive y component when x component is positive. One may determine which is better C_1 or C_3 by doing the least squares calculation using general $(h, k, l \pm n\delta)$ reflections. This formulation is, however, complicated as can be seen in Eqs. (6) and (7), and we used the criterion that the thiourea molecule should not be deformed drastically by the modulation wave. Table IV shows the (001) projection of the atomic distance calculated at the maximum displacement of modulation by using x_j , α_j , y_j , β_j listed in Table II for the combinations C_1 and C_3 , in comparison to the bond length at 20°C. It is clearly seen that C_1 gives

better agreement between the values at -86°C and 20°C than C_3 . Therefore, we decided that the values of φ_{xj} and φ_{yj} corresponding to the combination C_1 were realized in the crystal, and they are listed in Table II. The values of x_j and y_j in Table II may be compared to those at 20°C : $x_S=0.1148$, $x_C=-0.1635$, $x_N=-0.2773$, $y_S=-0.0073$, $y_C=0.0906$, $y_N=0.1307$.⁵⁾

Figure 7 shows the maximum atomic displacements caused by the modulation referring to the atomic positions in the unperturbed structure at -86°C . The values of α_j and β_j listed in Table II and demonstrated in Fig. 7 show that the displacement of the molecule is translation-like along the a axis.

As mentioned above, the structural modulation destroys the n-glide symmetry and thus the centre of symmetry locally, and results in the polarization wave in the crystal. The b-glide symmetry which we assume to exist even in the modulated structure has its reflection plane perpendicular to the a axis. Also it is assumed that z-parameters are not modulated. Therefore, the polarization of each unit cell caused by the structural modulation should be parallel to the b axis. Figure 8 shows the modulation wave and the polarization wave schematically.

§6 Temperature Dependence of Modulation Parameters

The temperature dependence of integrated intensities of several $(h, 0, n\delta)$, $(0, k, n\delta)$ reflections were measured by means of a single crystal diffractometer. These intensities vary continuously and monotonically in the temperature range which covers the phases II, III and IV.

Results of the measurements are shown by circles in Figs. 9 and 10. As seen in Figs. 9 and 10, integrated intensities of $(0, 2, \delta)$, $(0, 4, \delta)$ and $(0, 6, \delta)$ are approximately proportional to $(T_{IV-V} - T)$ and that of $(5, 0, \delta)$ is roughly proportional to $(T_{IV-V} - T)^2$ in the vicinity of T_{IV-V} , where T is temperature and T_{IV-V} is the transition point between the phases IV and V. The integrated intensity is proportional to $|F|^2$ and, as seen in Eq. (14), F of $(h, 0, \delta)$ can be approximated by the linear combination of α_j 's, if they are small, and in the same way, F of $(0, k, \delta)$ can be approximated by the linear combination of β_j 's. Therefore, the above-mentioned temperature dependence of $(h, 0, \delta)$ and $(0, k, \delta)$ reflections suggest that α_j is expressed as $a_j(T_{IV-V} - T)$ and β_j as $b_j(T_{IV-V} - T)^{1/2}$, where a_j and b_j are constants. The parameters α_j and β_j must have the values listed in Table II at -86°C , so that the coefficients a_j and b_j are determined as follows.

$$\left. \begin{aligned}
 \alpha_j &= a_j (T_{IV-V} - T) \\
 a_S &= 0.0008 \\
 a_C &= 0.0010 \\
 a_N &= 0.0013 \\
 \beta_j &= b_j (T_{IV-V} - T)^{1/2} \\
 b_S &= 0.0067 \\
 b_C &= 0.0015 \\
 b_N &= 0.0005
 \end{aligned} \right\} \quad (20)$$

Also from the data shown in Fig. 4, we have the expression of temperature dependence of M as

$$M = 8 + 0.0018(T_{IV-V} - T)^2 \quad (21)$$

The curve in Fig. 4 shows values calculated by this equation. The solid lines in Figs. 9 and 10 show results of the calculation based on Eqs. (9), (18), (20) and (21). In this calculation x_j and y_j are put equal to the values at -86°C , which are listed in Table II. The agreement between the observed and the calculated values is satisfactory for the satellite scatterings. Calculations proved that the satellite intensities were rather insensitive to the temperature dependence of x_j and y_j but intensities of the main scatterings were sensitive to it. The discrepancy between the observed and the calculated intensities of (020), (040) and (060) can be improved by assuming the temperature dependence of y_j , but it is difficult to avoid arbitrariness in determining temperature dependence of y_j and the details are not

described here. In the next section, brief discussion will be made on the implication of Eqs. (20).

§7 Discussion

In spite of the arbitrary assumption such as $\beta_{j1} = \beta_{j2}$ (Eq. (19)), we obtained the R factor of 0.16, which suggests that our model is not so far from reality.

As mentioned in §1, Tanisaki and Nakamura¹²⁾ and Futama¹³⁾ also made structural studies on the satellite scattering by thiourea. Atomic shifts caused by the structural modulation were calculated on the assumption similar to us, for -85°C by Tanisaki et al. and for -100°C by Futama. We have rewritten their formulations by using our notations and compared their results to ours in Table V. No numerical values are given to x_j and y_j in Futama's paper.¹³⁾ As described in §6, we assumed that x_j and y_j do not depend upon temperature, while α_j and β_j are functions of temperature as expressed by Eqs. (20). The values shown as "present study" in Table V are calculated on these assumptions for -85°C and -100°C . A similar trend can be observed between the results of Tanisaki et al. and ours. There is a somewhat large disagreement between the results of Futama and ours. To check reliability of our values

at -100°C , we took Weissenberg photograph of $(0, k, l + \delta)$ reflections at -100°C . Our parameters could explain the observed intensities of the satellites better than Futama's parameters. He used only $(0k0)$ and $(h00)$ reflections and satellites around them to determine his parameters. Large discrepancy between the values observed and calculated with his parameters were found on some satellite reflections around $(0kl)$ other than those around $(0k0)$. Tanisaki et al. introduced longitudinal component of modulation wave, and his final R factors were 0.17 for Bragg reflections, 0.18 for the first satellites and 0.21 for the second satellites. We observed no satellites around $(00l)$ reflections and assumed that the modulation was pure transverse wave. Our final value (0.16) of R is a little smaller than theirs.

In 1961, Tanisaki¹⁸⁾ found satellite x-ray scattering by NaNO_2 . Its characteristic features are that only the first satellites are present, a fact suggesting that the satellites are caused by the amplitude modulation.¹⁷⁾ Therefore, the satellite scattering by thiourea is a phenomenon quite different from that by NaNO_2 . Our results described in this paper suggest that the structural modulation in thiourea can be looked upon as a frozen-in of a transverse optical lattice vibration, as pointed out first by us.⁹⁾ This idea is schematically shown

in Fig. 11, which demonstrates that the angular frequency of an optical mode becomes zero at T_{IV-V} . In this connection, it may be worth-while to report that we observed diffuse x-ray scatterings extended along the c^* axis on the $(Ok\ell)$ reciprocal plane near the transition point T_{IV-V} .

The phase III is ferroelectric with the polar axis parallel to the b axis.²⁾ The spontaneous polarization should destroy the n -glide symmetry of the unperturbed structure. We tried to observe in the phase III the Bragg reflection $(h0\ell)$ with $h+\ell=\text{odd}$, which should be present if the n -glide is destroyed, but we did not succeed in it. Also intensities of the main and satellite scatterings vary monotonically in the temperature range which covers the phases II, III and IV. These facts seem to be related to the very small value of the spontaneous polarization in phase III as small as 10^{-3} times of P_S in the phase I. Possibly this small magnitude of P_S permits the coexistence of the structural modulation and the spontaneous polarization in the phase III.

As is well known, in case of ferroelectric phase transition of second order, the usual phenomenological theory gives the temperature dependence of the spontaneous polarization P_S as $P_S \propto (T_C - T)^{1/2}$, where T_C is the Curie temperature. The spontaneous electrostriction which is proportional to P_S^2 is thus proportional to $(T_C - T)$.

In this connection it is interesting to observe that the parameters β_j which are linearly related to the polarization wave when they are small are proportional to $(T_{IV-V}-T)^{1/2}$ and that the parameters α_j which are linearly related to atomic shifts perpendicular to the polarization direction are proportional to $(T_{IV-V}-T)$, as given by Eqs. (20).

Acknowledgements

The author wishes to express his sincere thanks to Professor T. Mitsui and Professor E. Nakamura for their encouragements and for many useful discussions.

References

- 1) A. L. Solomon: Phys. Rev. 104 (1956) 1191.
- 2) G. J. Goldsmith and J. G. White: J. Chem. Phys. 31 (1959) 1175.
- 3) N. R. Kunchur and M. R. Truter: J. Chem. Soc. (1958) 2551.
- 4) M. R. Truter: Acta Cryst. 22 (1967) 556.
- 5) M. M. Elcombe and J. C. Taylor: Acta Cryst. A24 (1968) 410.
- 6) C. Calvo: J. Chem. Phys. 33 (1960) 1721.
- 7) H. Futama: J. Phys. Soc. Japan 17 (1962) 434.
- 8) H. Futama and A. Chiba: Reported at Annual Meeting of the Physical Society of Japan, held in Fukuoka, October in 1963.
- 9) T. Mitsui, E. Nakamura, Y. Shiozaki, H. Motegi, T. Sekido, M. Ichikawa, T. Takama, M. Hosoya, K. Shibukawa, N. Wakaki and J. Furuichi: Proc. Intern. Meeting on Ferroelectricity, Prague, 1966, Vol. 1, p.222.
- 10) H. Futama, Y. Shiozaki, A. Chiba, E. Tanaka, T. Mitsui and J. Furuichi: Phys. Letters 25A (1967) 8.
- 11) Y. Shiozaki and M. Hosoya: J. Phys. Soc. Japan 38 Suppl. (1970) 290.
- 12) S. Tanisaki and N. Nakamura: J. Phys. Soc. Japan 28 Suppl. (1970) 293.

- 13) H. Futama: J. Phys. Soc. Japan 28 Suppl. (1970)
295.
- 14) A. Guinier: X-Ray Diffraction (W. H. Freeman and
Company, San Francisco and London, 1963).
- 15) A. J. C. Wilson: X-Ray Optics (Methuen, London,
1962).
- 16) M. Korekawa: Nihon Kesshō Gakkai-shi 6 (1964) 2.
(in Japanese)
- 17) Y. Yamada, I. Shibuya and S. Hoshino: J. Phys. Soc.
Japan 18 (1963) 1594.
- 18) S. Tanisaki: J. Phys. Soc. Japan 16 (1961) 579.

Figure Captions

- Fig. 1. Dielectric constants of thiourea as a function of temperature and five phases (after Goldsmith and White²).
- Fig. 2. Weissenberg photograph of $(0k\ell)$ reflections taken at -100°C .
- Fig. 3. Distribution of satellite scatterings. Strong reflections are represented by large spots.
 (a) Around $(0k\ell)$ Bragg reflections.
 (b) Around $(h0\ell)$ Bragg reflections.
- Fig. 4. $1/\delta$ vs. temperature. Later $1/\delta$ will be denoted as M (Eq. (2)). Circles stand for values determined by the diffractometer and the curve shows values calculated by Eq. (21).
- Fig. 5. Unit cell of the unperturbed structure of thiourea. The space group is $Pbnm$. Atoms S and C are on mirror planes. Each nitrogen atom in $2N$ is a mirror image of the other with respect to the mirror plane.
- Fig. 6. Unit cell of thiourea when the modulation is introduced. For detailed explanation, see text.
- Fig. 7. Atomic shifts caused by the modulation at -86°C . Projection on (001) plane is shown. The number assigned to each atom is the same as

in Figs. 5 and 6. Molecules at the positions of the maximum displacements are drawn with solid lines. Molecules at their positions in the unperturbed structure are drawn by broken lines.

Fig. 8. Illustration of the modulated structure projected on (100) over the full wave length M_c of the modulation.

(a) Atoms S and C of thiourea molecule lie on the planes at $z=1/4$ or $3/4$ and its (100) projection is as shown in the upper figure, which is represented by the arrow shown in the lower figure.

(b) Structural modulation over ten unit cell aligned along the c axis. Arrows directed to right and to left correspond to the molecules 1 and 4 in Fig. 7, respectively. The period M is equal to 8.4 here, which is the value at -86°C . In this drawing, the ratio of the lengths of the molecule and the c axis does not correspond to the actual value.

(c) Polarization of each unit cell caused by the structural modulation. The polarization is parallel or antiparallel to the b axis.

Fig. 9. Integrated intensities I of $(0, k, n\delta)$ reflections as functions of temperature, in electron unit.

Circles represent experimental data and the solid curves to the values calculated based upon Eqs. (20) and (21). (a) Reflections around (020). (b) Reflections around (040). (c) Reflections around (060).

Fig. 10. Integrated intensity I of (506) reflection as a function of temperature, in electron unit. Circles represent experimental data and the solid curve to the values calculated based upon Eqs. (20) and (21).

Fig. 11. Proposed temperature dependence of the dispersion relation for a transverse optical branch of lattice vibration. The propagation vector \underline{q} is parallel to the c^* axis and ω is the angular frequency. The structurally modulated phase IV takes place when ω becomes zero at $\underline{q} = 2\pi\underline{c}^*/M$, as shown by the lower curve.

Table I. Values of the parameters which were fixed constants in least squares calculation.

$$\text{Temperature factor} = \exp(-b_{11}h^2 - b_{22}k^2 - b_{33}l^2 - 2b_{12}hk - 2b_{13}hl - 2b_{23}kl).$$

z_j	b_{11}	b_{22}	b_{33}	b_{12}	b_{13}	b_{23}
S	0.2500	0.0101	0.0148	0.0059	-0.0011	0.0000
C	0.2500	0.0153	0.0098	0.0053	0.0025	0.0000
N	0.1171	0.0262	0.0192	0.0061	0.0100	0.0007

M=8.4

Table II. Parameters at -86°C determined by the least squares calculation. Parameters x_j and y_j represent the atomic positions in the unperturbed structure, and parameters α_j , β_j and φ_{xj} , φ_{yj} are amplitudes and phases of the modulation wave, respectively.

	x_j	α_j	φ_{xj}	y_j	β_j	φ_{yj}
S	0.115	0.012	0.5	-0.009	0.026	0
C	-0.165	0.015	0.5	0.106	0.006	0
N	-0.292	0.019	0.5	0.131	0.002	0.5

Table III(a). Absolute values of observed and calculated structure amplitudes of $(h,0,l-n\delta)$ reflections. $F_o(n)$: observed, $F_c(n)$: calculated, $\Delta F(n) \equiv |F_o(n)| - |F_c(n)|$. Here $n=0$ corresponds to the main Bragg reflection and $n=1$ to the first satellite at $(h,0,l-\delta)$.

h	k	l	$F_o(0)$	$F_c(0)$	$\Delta F(0)$	$F_o(1)$	$F_c(1)$	$\Delta F(1)$
1	0	0	0.0	0.0	0.0	1.5	1.4	0.1
1	0	1	13.3	13.9	-0.6	0.0	0.3	-0.3
1	0	2	0.0	0.0	0.0	2.7	1.8	0.9
1	0	3	34.4	45.2	-10.8	0.0	0.4	-0.4
1	0	4	0.0	0.0	0.0	2.8	1.7	1.1
1	0	5	24.4	23.0	1.4	0.0	0.3	-0.3
1	0	6	0.0	0.0	0.0	0.0	0.9	-0.9
1	0	7	3.0	1.4	1.6	0.0	0.1	-0.1
1	0	8	0.0	0.0	0.0	0.0	0.5	-0.5
1	0	9	7.6	4.1	3.5	0.0	0.1	-0.1
1	0	10	0.0	0.0	0.0	0.0	0.5	-0.5
2	0	0	33.4	35.6	-2.2	0.0	0.9	-0.9
2	0	1	0.0	0.0	0.0	4.2	3.9	0.3
2	0	2	6.5	4.7	1.8	0.0	0.4	-0.4
2	0	3	0.0	0.0	0.0	0.0	0.7	-0.7
2	0	4	19.0	17.0	2.0	0.0	0.1	-0.1
2	0	5	0.0	0.0	0.0	0.0	0.9	-0.9
2	0	6	4.3	3.0	1.3	0.0	0.3	-0.3
2	0	7	0.0	0.0	0.0	2.9	1.8	1.1
2	0	8	6.2	7.8	-1.6	0.0	0.3	-0.3
2	0	9	0.0	0.0	0.0	0.0	1.1	-1.1
2	0	10	3.8	2.9	0.9	0.0	0.1	-0.1
3	0	0	0.0	0.0	0.0	2.7	0.4	2.3
3	0	1	37.5	41.3	-3.8	0.0	0.3	-0.3
3	0	2	0.0	0.0	0.0	5.4	3.6	1.8
3	0	3	17.7	15.0	2.7	0.0	1.1	-1.1
3	0	4	0.0	0.0	0.0	7.5	5.3	2.2
3	0	5	19.0	16.7	2.3	0.0	0.8	-0.8
3	0	6	0.0	0.0	0.0	3.1	2.0	1.1
3	0	7	23.0	23.4	-0.4	0.0	0.2	-0.2
3	0	8	0.0	0.0	0.0	1.7	0.6	1.1
3	0	9	13.1	13.9	-0.8	0.0	0.2	-0.2
4	0	0	24.2	25.2	-1.0	0.0	0.3	-0.3
4	0	1	0.0	0.0	0.0	0.0	0.6	-0.6
4	0	2	30.9	34.8	-3.9	0.0	0.5	-0.5
4	0	3	0.0	0.0	0.0	6.0	4.9	1.1
4	0	4	36.4	36.0	0.4	0.0	1.0	-1.0
4	0	5	0.0	0.0	0.0	4.1	3.6	0.5
4	0	6	21.7	22.2	-0.5	0.0	0.3	-0.3
4	0	7	0.0	0.0	0.0	0.0	0.3	-0.3
4	0	8	13.1	14.2	-1.1	0.0	0.1	-0.1
5	0	0	0.0	0.0	0.0	8.4	8.8	-0.4
5	0	1	12.5	9.5	3.0	0.0	1.5	-1.5
5	0	2	0.0	0.0	0.0	3.3	4.1	-0.8
5	0	3	5.5	3.1	2.4	0.0	0.2	-0.2
5	0	4	0.0	0.0	0.0	0.0	0.1	-0.1
5	0	5	6.1	3.5	2.6	0.0	0.3	-0.3
5	0	6	0.0	0.0	0.0	3.7	3.5	0.2
5	0	7	9.0	6.0	3.0	0.0	1.0	-1.0
6	0	0	7.2	3.8	3.4	0.0	0.1	-0.1
6	0	1	0.0	0.0	0.0	2.4	1.8	0.6
6	0	2	4.6	3.6	1.0	0.0	1.0	-1.0
6	0	3	0.0	0.0	0.0	6.2	8.1	-1.9
6	0	4	3.3	2.9	0.4	0.0	1.7	-1.7
6	0	5	0.0	0.0	0.0	4.9	6.5	-1.6

Table III(b). Absolute values of observed and calculated structure amplitude of $(0, k, \ell - n\delta)$ reflections.

Here $n=2$ corresponds to the second satellite at $(0, k, \ell - 2\delta)$. Other notations are the same as in Table III(a)

h	k	ℓ	$F_o(0)$	$F_c(0)$	$\Delta F(0)$	$F_o(1)$	$F_c(1)$	$\Delta F(1)$	$F_o(2)$	$F_c(2)$	$\Delta F(2)$
0	2	0	47.0	47.7	-0.7	9.5	8.3	1.2	0.0	0.7	-0.7
0	2	1	36.3	40.6	-4.3	0.0	0.9	-0.9	0.0	0.2	-0.2
0	2	2	39.4	44.5	-5.1	6.6	7.1	-0.5	0.0	0.6	-0.6
0	2	3	16.7	18.3	-1.6	0.0	1.3	-1.3	0.0	0.2	-0.2
0	2	4	32.2	37.2	-5.0	5.1	5.2	-0.1	0.0	0.4	-0.4
0	2	5	4.8	5.2	-0.4	0.0	0.9	-0.9	0.0	0.1	-0.1
0	2	6	21.1	24.0	-2.9	3.7	4.0	-0.3	0.0	0.3	-0.3
0	2	7	10.7	13.6	-2.9	3.0	3.0	-0.4	0.0	0.1	-0.1
0	2	8	16.0	17.4	-1.4	0.0	0.4	-0.4	0.0	0.1	-0.1
0	2	9	2.8	5.0	-2.2	0.0	0.3	-0.3	0.0	0.2	-0.2
0	2	10	11.0	12.9	-1.9	2.9	2.0	-0.9	0.0	0.1	-0.1
0	4	0	4.3	4.3	0.0	9.5	9.2	0.3	2.7	2.7	0.0
0	4	1	1.3	4.5	-3.2	1.8	0.1	1.5	0.0	1.3	-0.3
0	4	2	21.4	19.4	2.0	8.0	8.0	0.0	1.7	1.7	0.0
0	4	3	4.0	4.5	-0.5	0.8	0.2	0.6	0.0	0.2	-0.2
0	4	4	26.8	27.4	-0.6	5.0	6.4	-0.6	1.6	1.2	0.4
0	4	5	3.4	9.0	-5.6	0.2	0.1	-0.1	0.0	0.2	-0.2
0	4	6	9.8	9.0	0.8	6.0	5.5	0.7	0.0	1.0	-1.0
0	4	7	1.8	2.2	-0.4	0.4	0.3	0.1	0.0	0.2	-0.2
0	4	8	4.0	1.1	2.9	4.0	4.3	-0.3	0.0	0.7	-0.7
0	4	9	0.0	1.8	-1.8	0.0	0.0	0.0	0.0	0.1	-0.1
0	4	10	6.2	11.4	-5.2	2.8	2.9	-0.4	3.6	3.0	0.6
0	6	0	12.6	11.3	1.3	8.5	7.2	1.2	0.0	2.0	-1.6
0	6	1	14.2	14.0	0.2	3.8	7.4	-1.8	2.5	0.1	-0.1
0	6	2	11.4	9.0	2.4	2.5	1.4	1.1	0.0	1.9	-0.6
0	6	3	2.8	1.5	1.3	6.6	1.7	4.9	2.0	0.1	-0.1
0	6	4	2.8	3.9	-1.1	2.6	6.4	-3.8	2.2	1.7	-0.5
0	6	5	2.8	3.9	-1.1	5.6	1.4	4.2	0.0	0.1	-0.1
0	6	6	2.8	3.9	-1.1	2.2	5.1	-2.9	0.0	1.4	-0.1
0	6	7	5.7	9.5	-3.8	1.4	1.4	0.0	1.7	0.0	0.0
0	6	8	2.0	4.6	-2.6	4.8	3.1	1.7	0.0	1.1	-0.1
0	6	9	2.0	4.6	-2.6	5.4	1.7	3.7	1.0	0.1	-0.1
0	6	10	2.0	4.6	-2.6	3.7	1.4	2.3	0.0	0.1	-0.1
0	8	0	3.7	3.7	0.0	3.7	4.8	-1.1	1.3	0.0	0.0
0	8	1	3.7	3.7	0.0	5.1	3.8	1.3	0.0	1.7	-0.7
0	8	2	3.7	3.7	0.0	0.0	0.8	-0.8	1.0	0.0	0.0
0	8	3	3.7	3.7	0.0	3.4	1.2	2.2	0.0	1.8	-0.8
0	8	4	3.7	3.7	0.0	5.7	1.4	4.3	0.0	0.1	-0.1
0	8	5	3.7	3.7	0.0	2.7	1.4	1.3	0.0	0.1	-0.1
0	8	6	3.7	3.7	0.0	5.2	1.4	3.8	0.0	0.1	-0.1
0	8	7	3.7	3.7	0.0	3.4	1.4	2.0	0.0	1.6	-0.6
0	8	8	3.7	3.7	0.0	5.2	1.4	3.8	0.0	0.1	-0.1
0	8	9	3.7	3.7	0.0	3.4	1.4	2.0	0.0	1.6	-0.6
0	8	10	3.7	3.7	0.0	5.2	1.4	3.8	0.0	0.1	-0.1

Table IV. Projection of interatomic distances on (001) in Å. The values at -86°C correspond to those at the maximum displacements caused by the modulation.

	At -86°C		At 20°C
	(Phase IV)		(Phase V)
	c_1	c_3	
S-C	1.72	1.87	1.71
C-N	0.72	0.77	0.70
S-N	2.44	2.62	2.41

Table V. Comparison of the parameters obtained in the present study and those by other authors. The parameters at -85°C and -100°C in the present study were calculated by using Eqs. (20).

	Present study, at -85°C						Tanisaki and Nakamura, at -85°C					
	x_j	α_j	ψ_{xj}	y_j	β_j	ψ_{yj}	x_j	α_j	ψ_{xj}	y_j	β_j	ψ_{yj}
S	0.115	0.011	0.5	-0.009	0.025	0	0.117	0.014	0.5	-0.006	0.026	0
C	-0.165	0.014	0.5	0.106	0.006	0	-0.165	0.029	0.5	0.091	0.007	0
N	-0.292	0.018	0.5	0.131	0.002	0.5	-0.278	0.034	0.5	0.129	0.002	0.5
	Present study, at -100°C						Futama, at -100°C					
	x_j	α_j	ψ_{xj}	y_j	β_j	ψ_{yj}	x_j	α_j	ψ_{xj}	y_j	β_j	ψ_{yj}
S	0.115	0.023	0.5	-0.009	0.036	0	—	0.013	0.5	—	0.021	0
C	-0.165	0.029	0.5	0.106	0.008	0	—	0.024	0.5	—	0.0385	0
N	-0.292	0.038	0.5	0.131	0.003	0.5	—	0.031	0.5	—	0.013	0

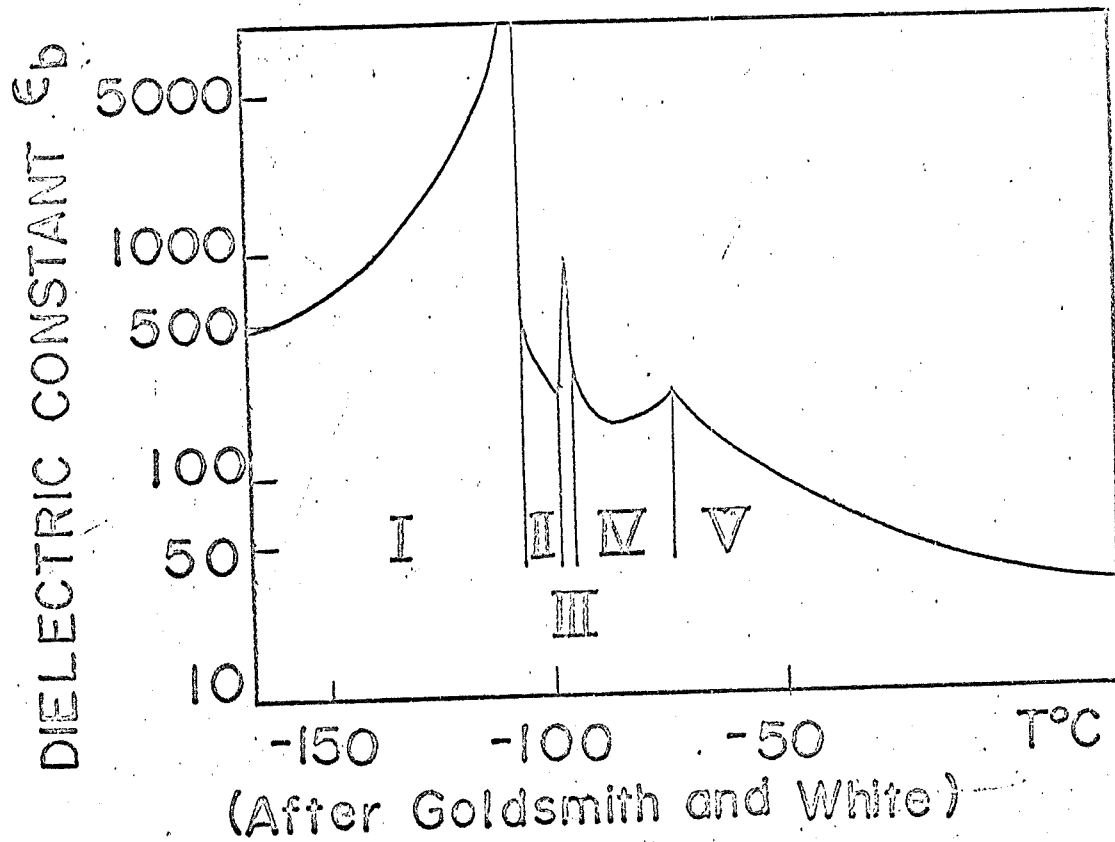


Fig. 1.

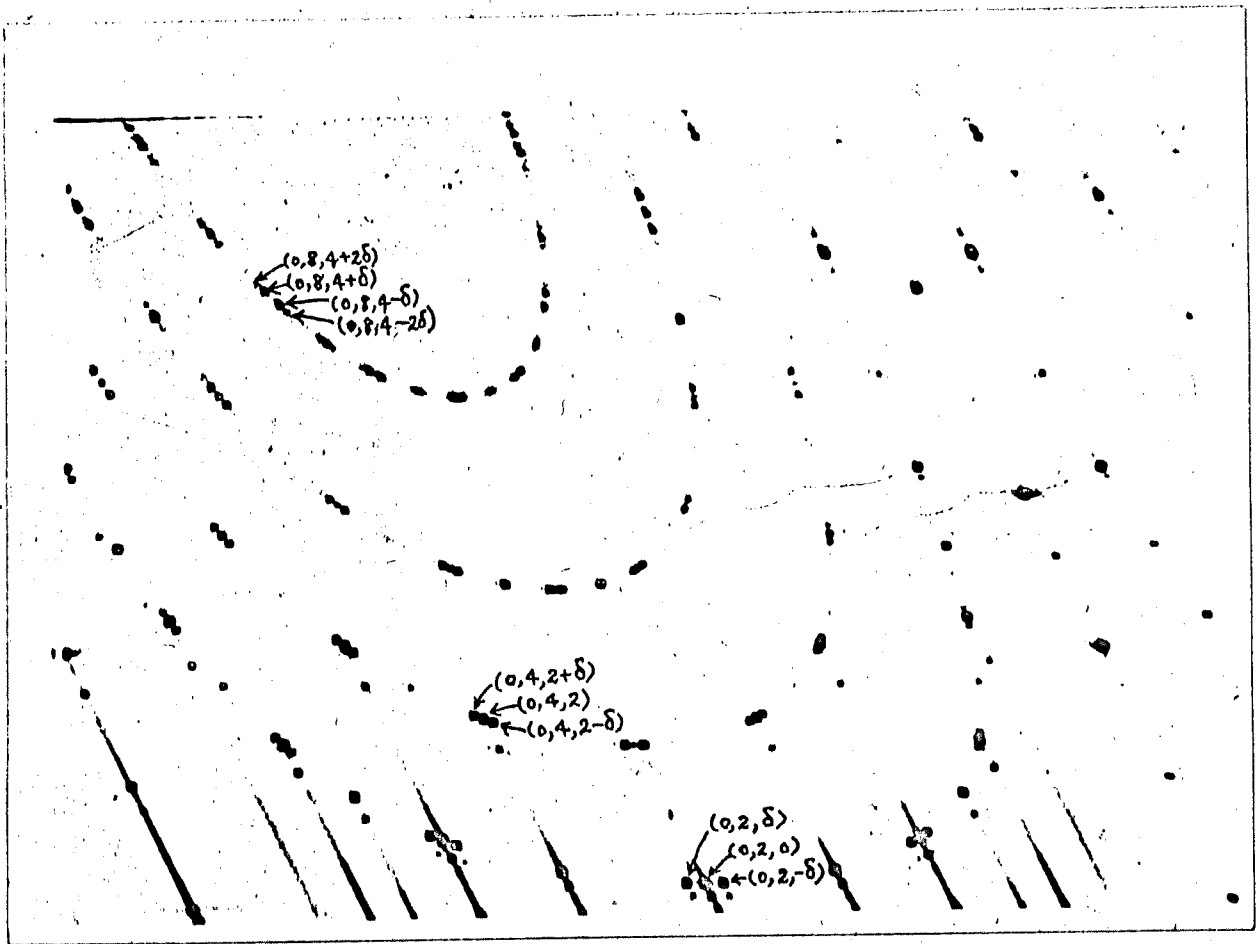


Fig. 2.

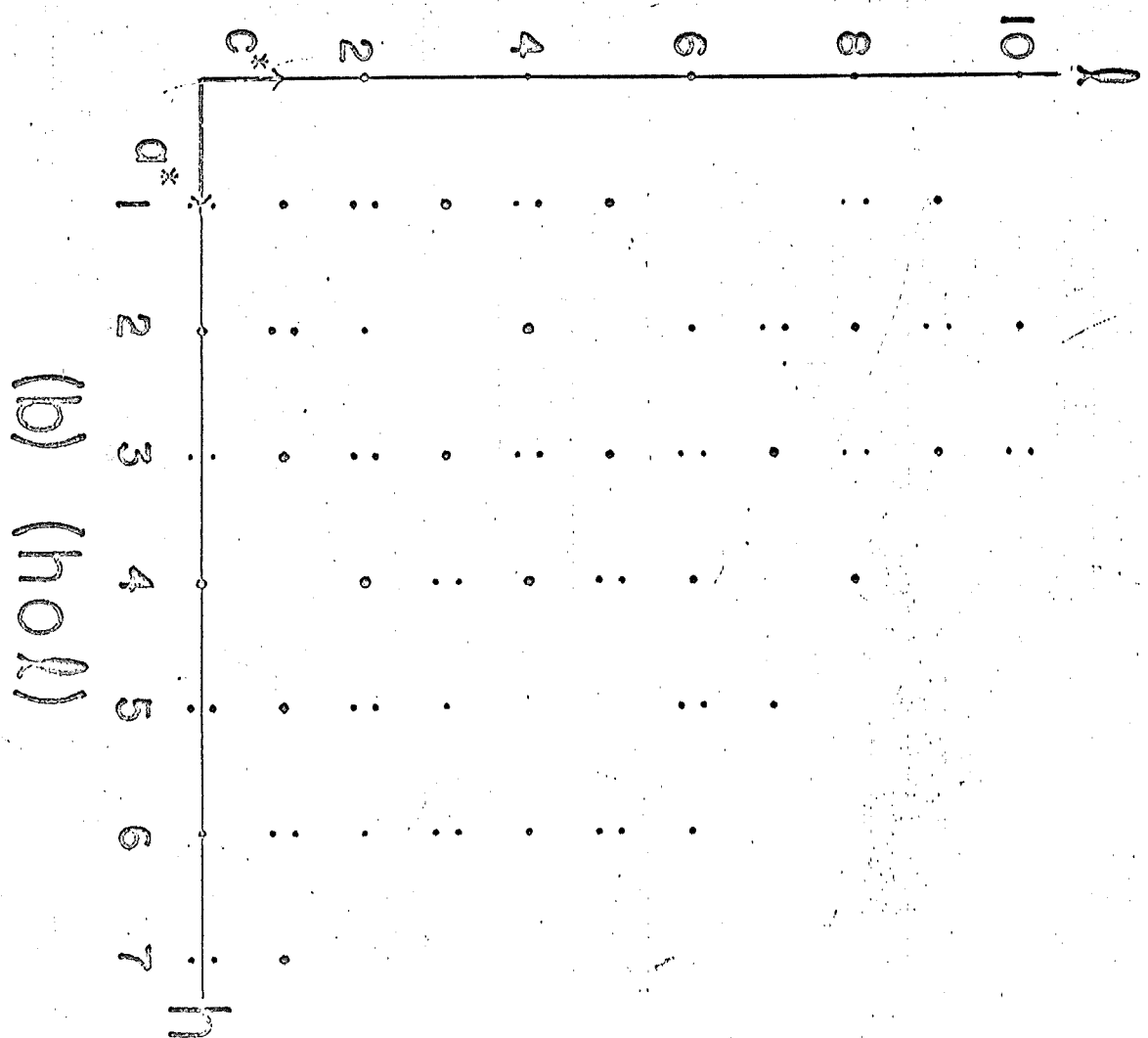
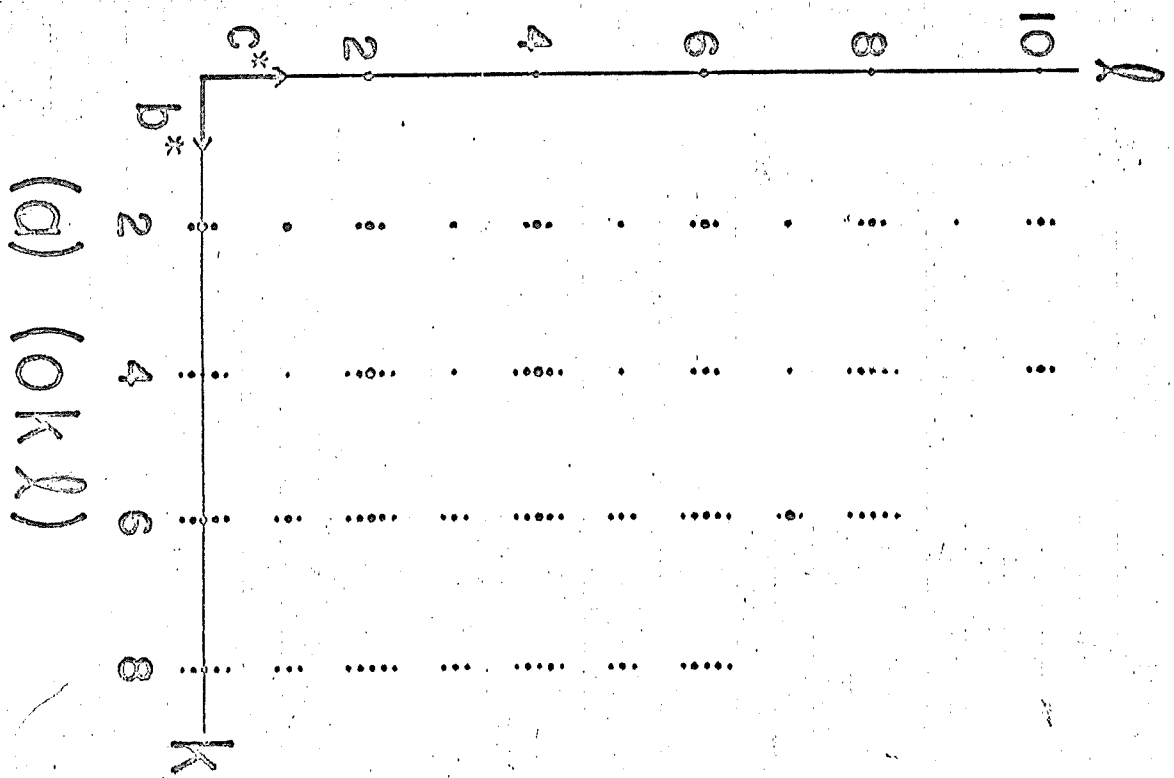


Fig. 3(a), (b).

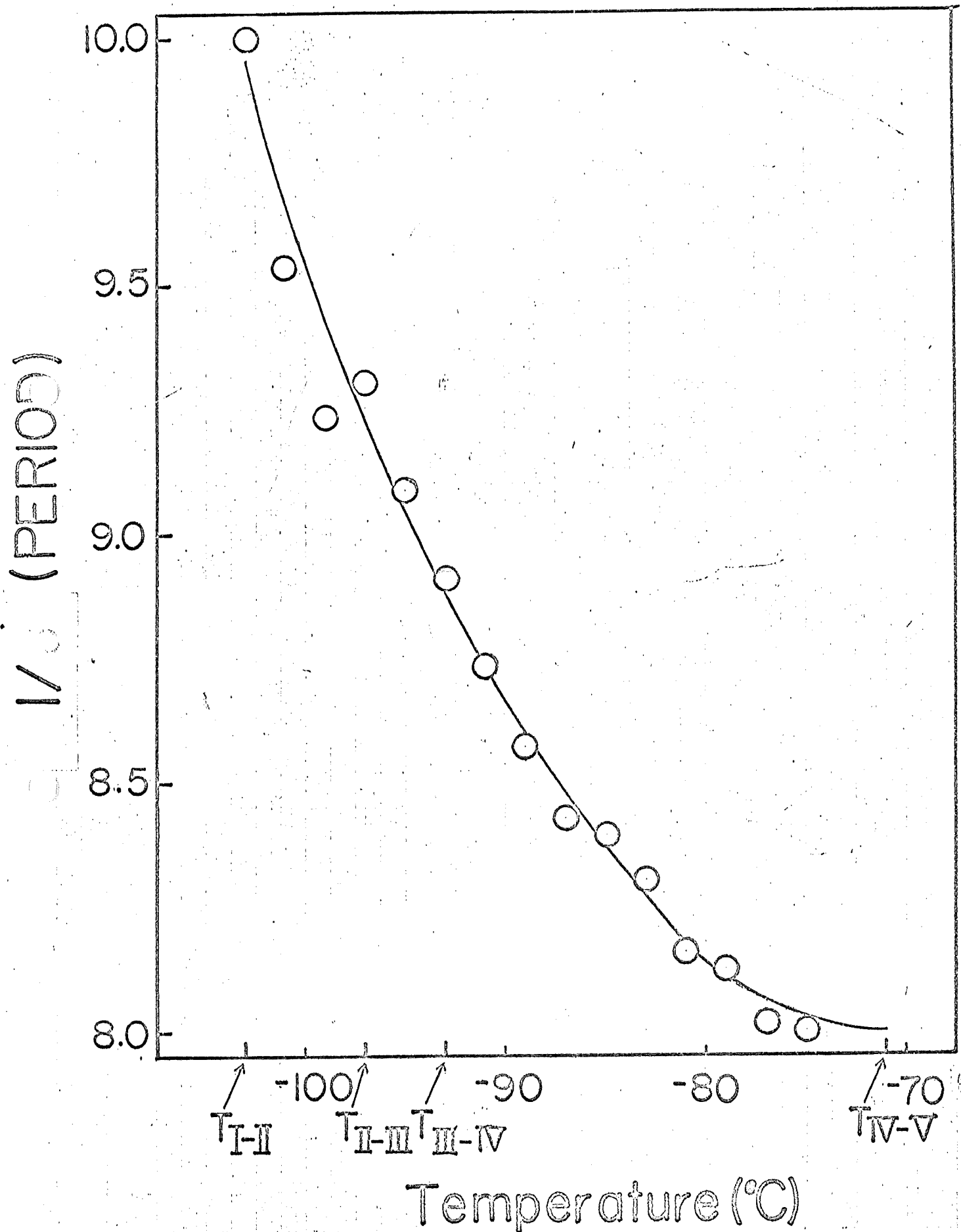


Fig. 4.

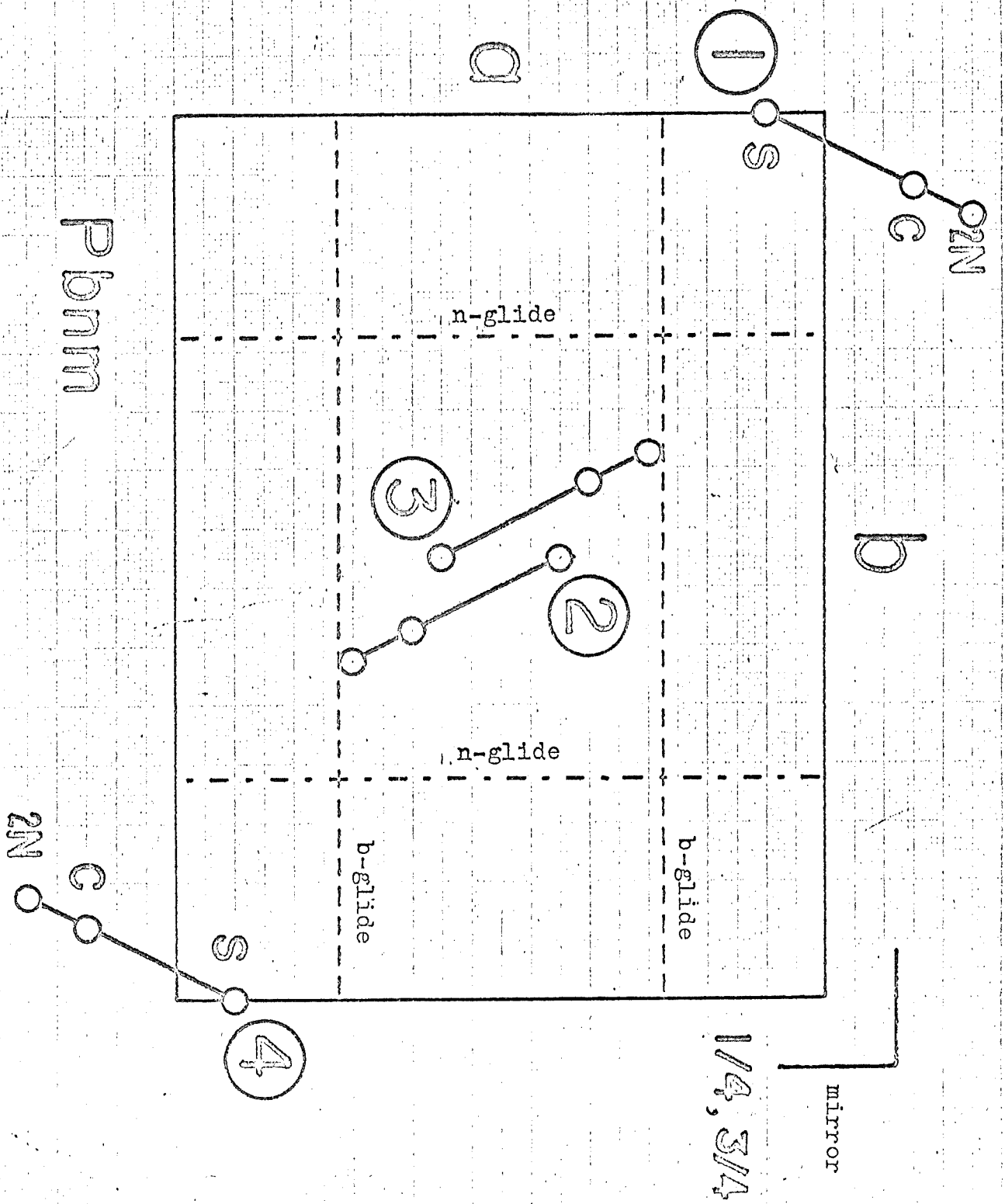
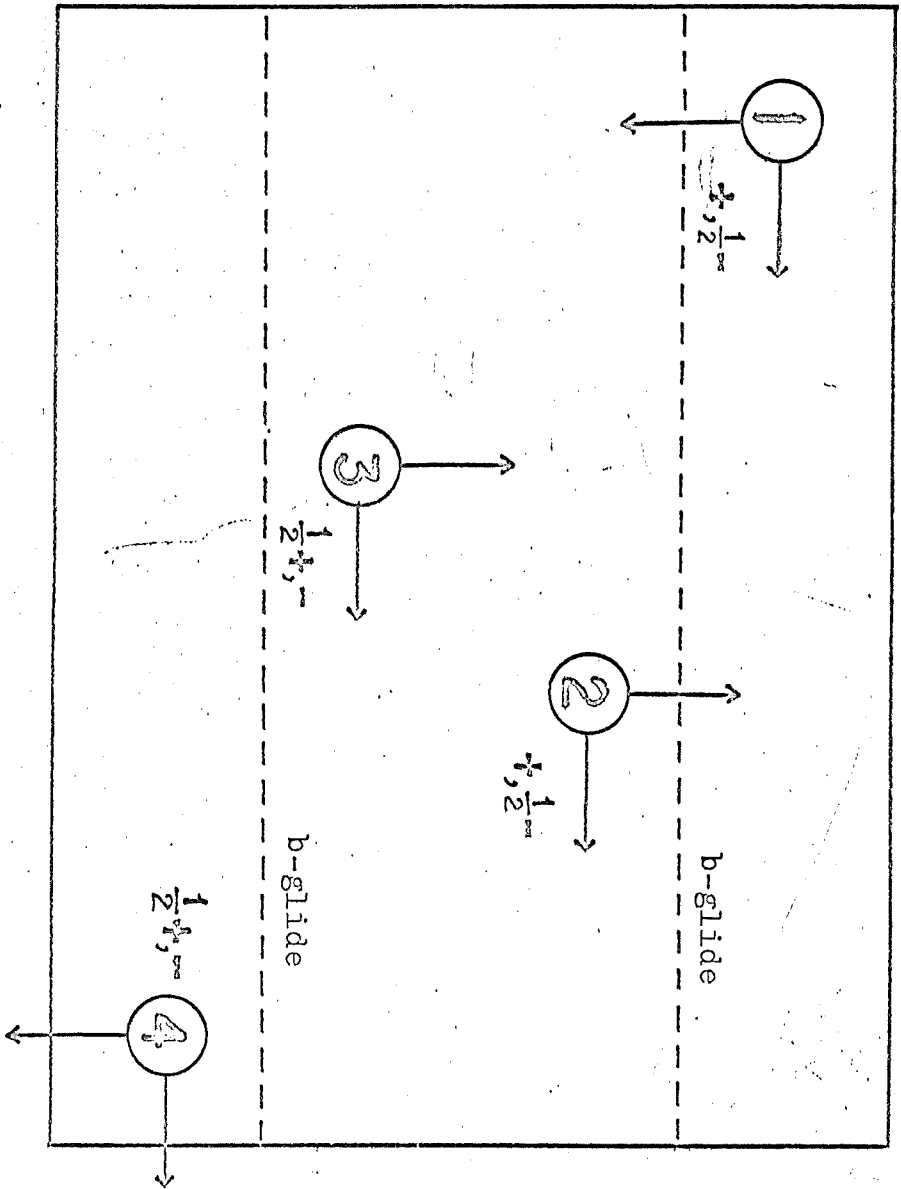


Fig. 5.

b



D

Fig. 6.

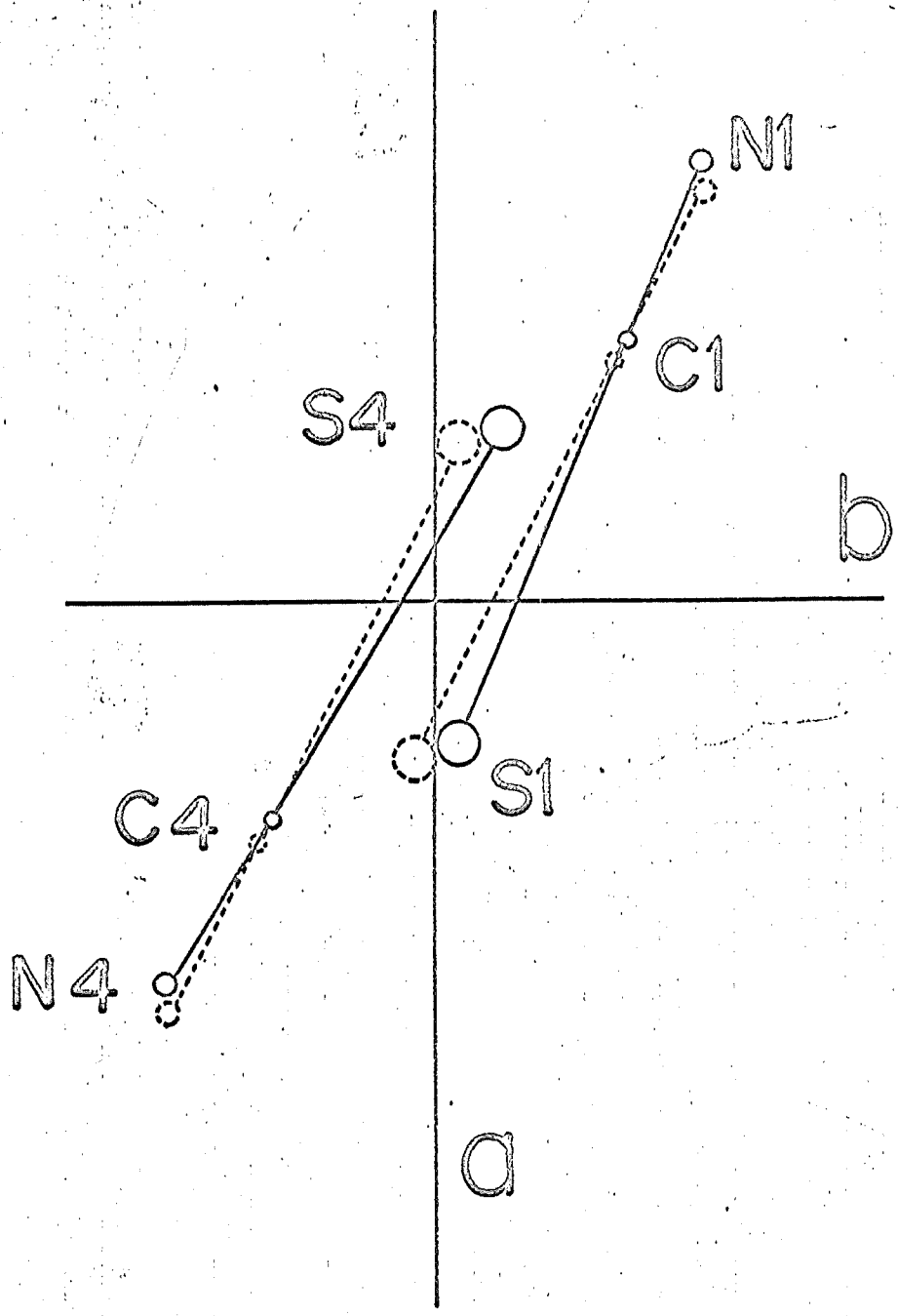
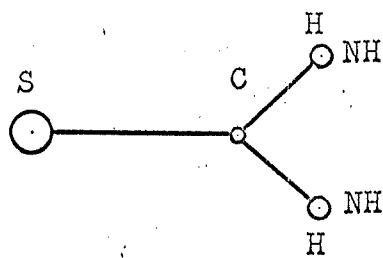
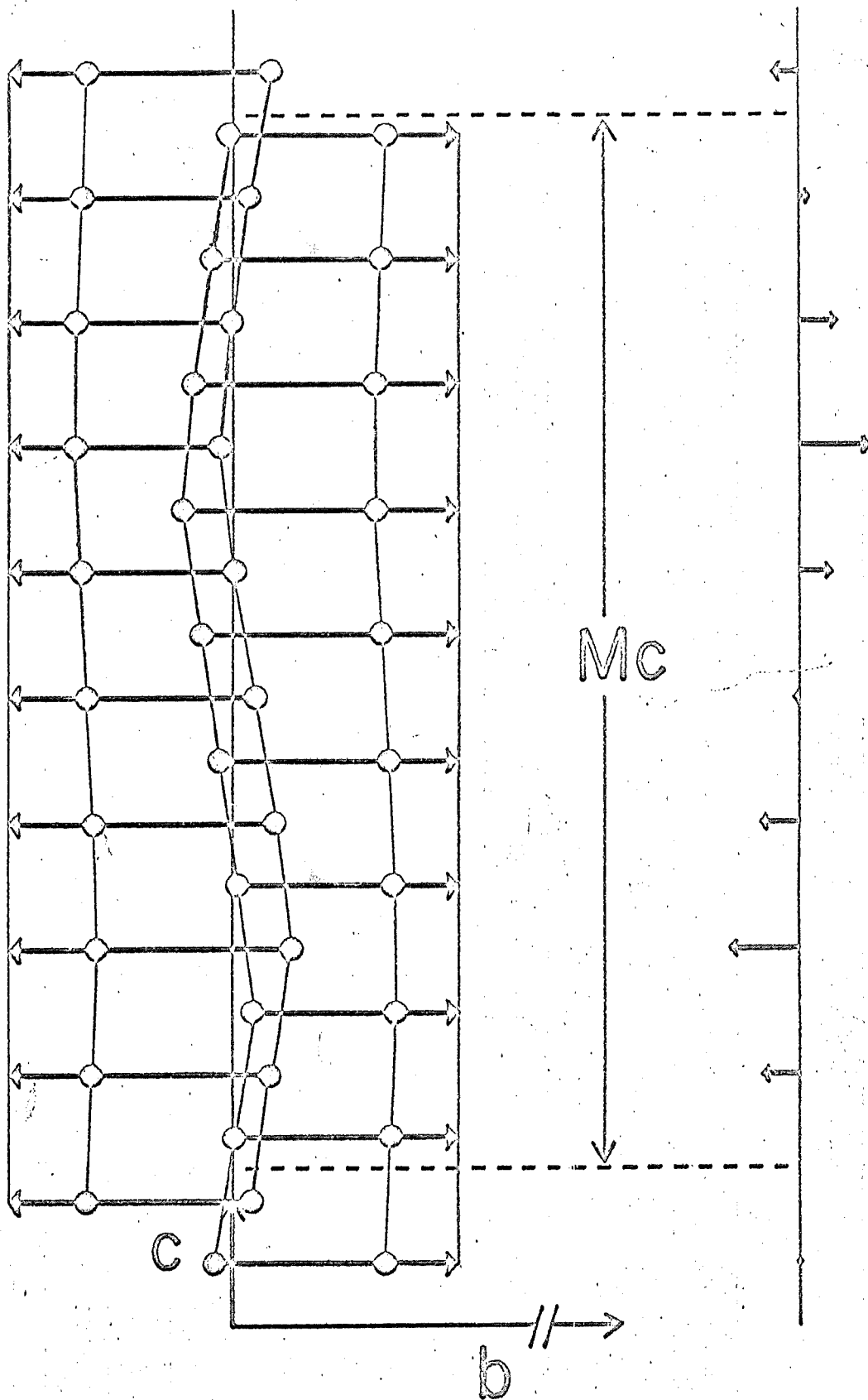


Fig. 7.



(a)

Fig. 8(a).



(b)

(c)

Fig. 8(b), (c).

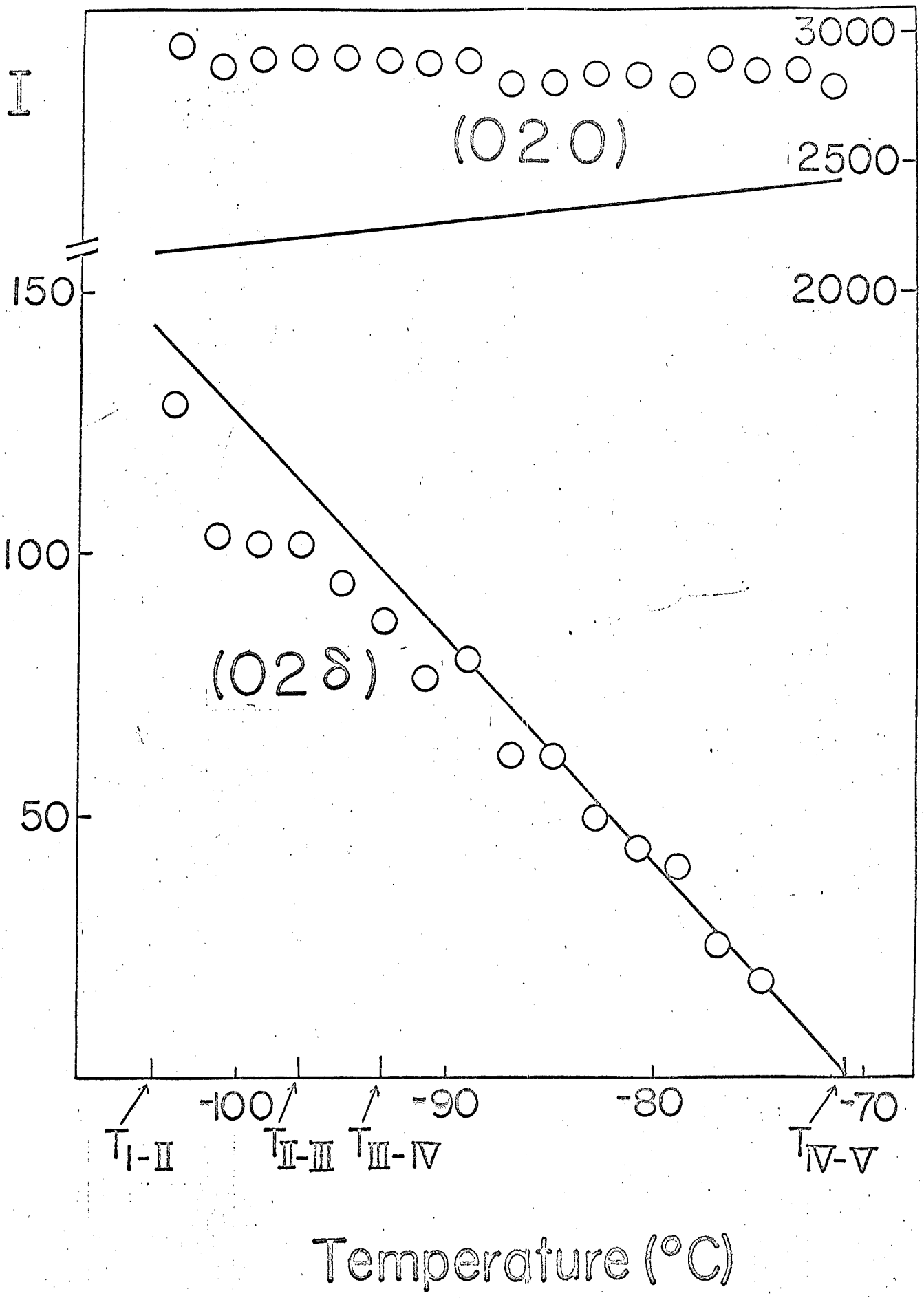


Fig. 9(a).

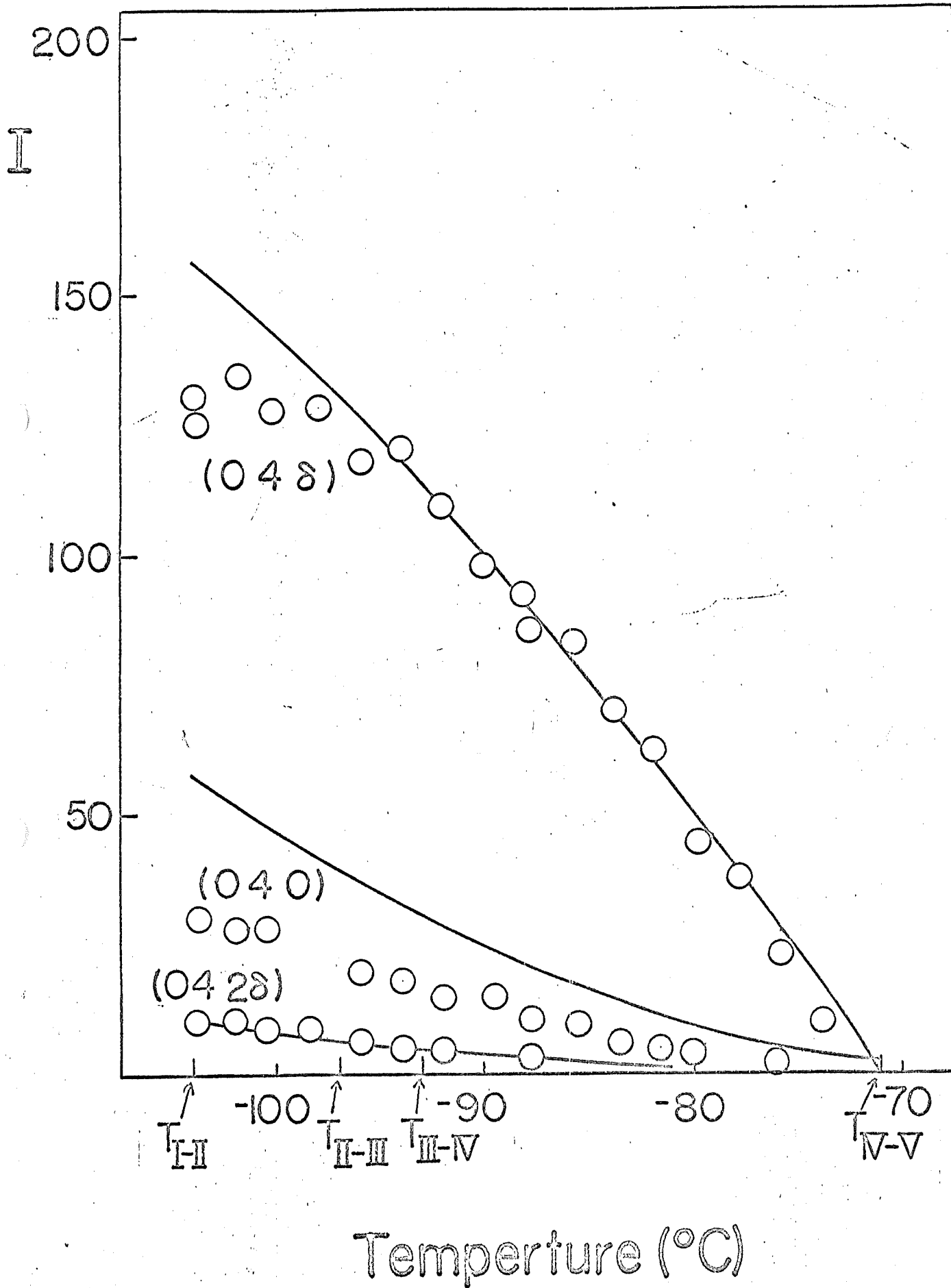


Fig. 9(b).

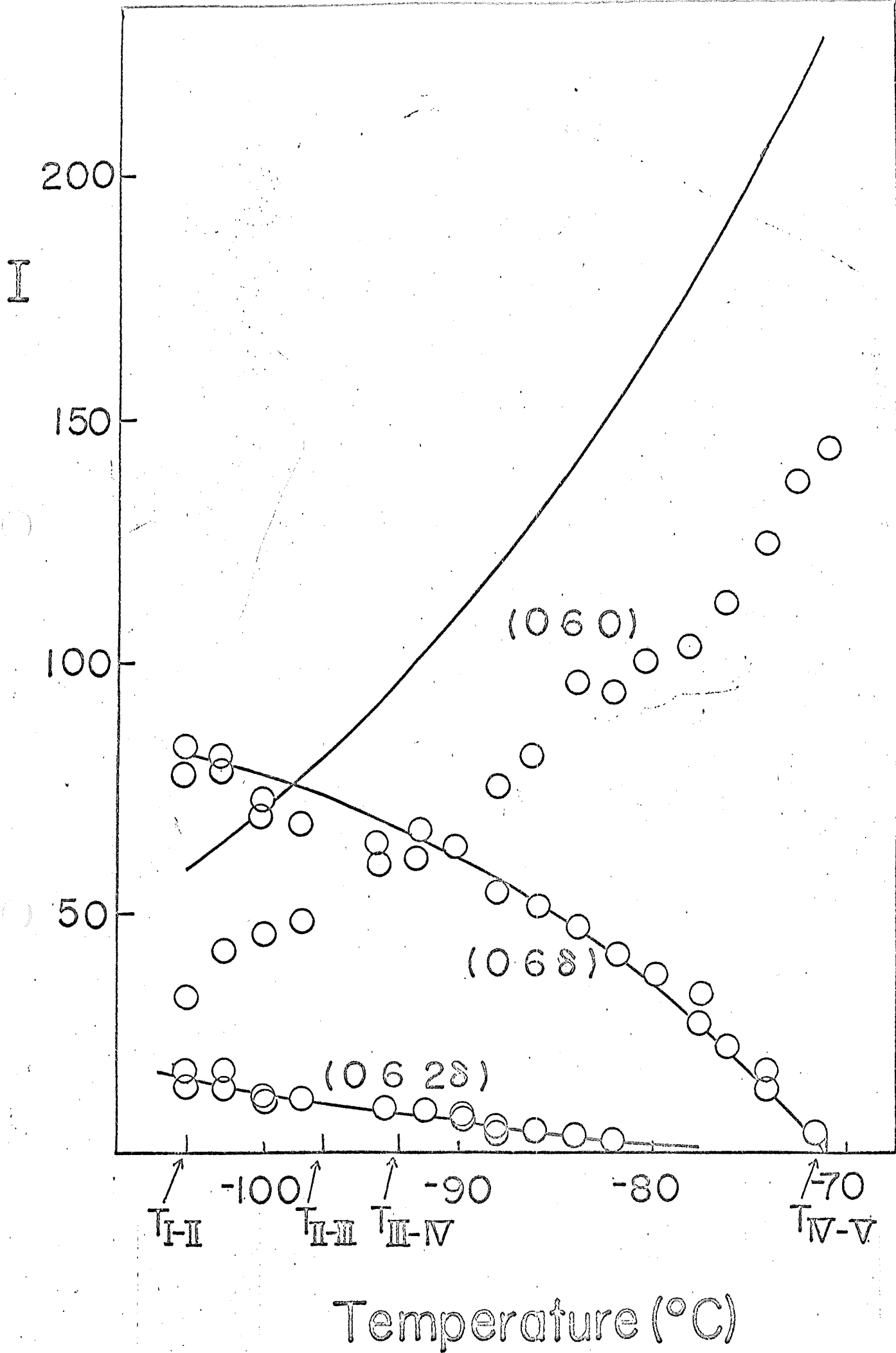


Fig. 9(c).

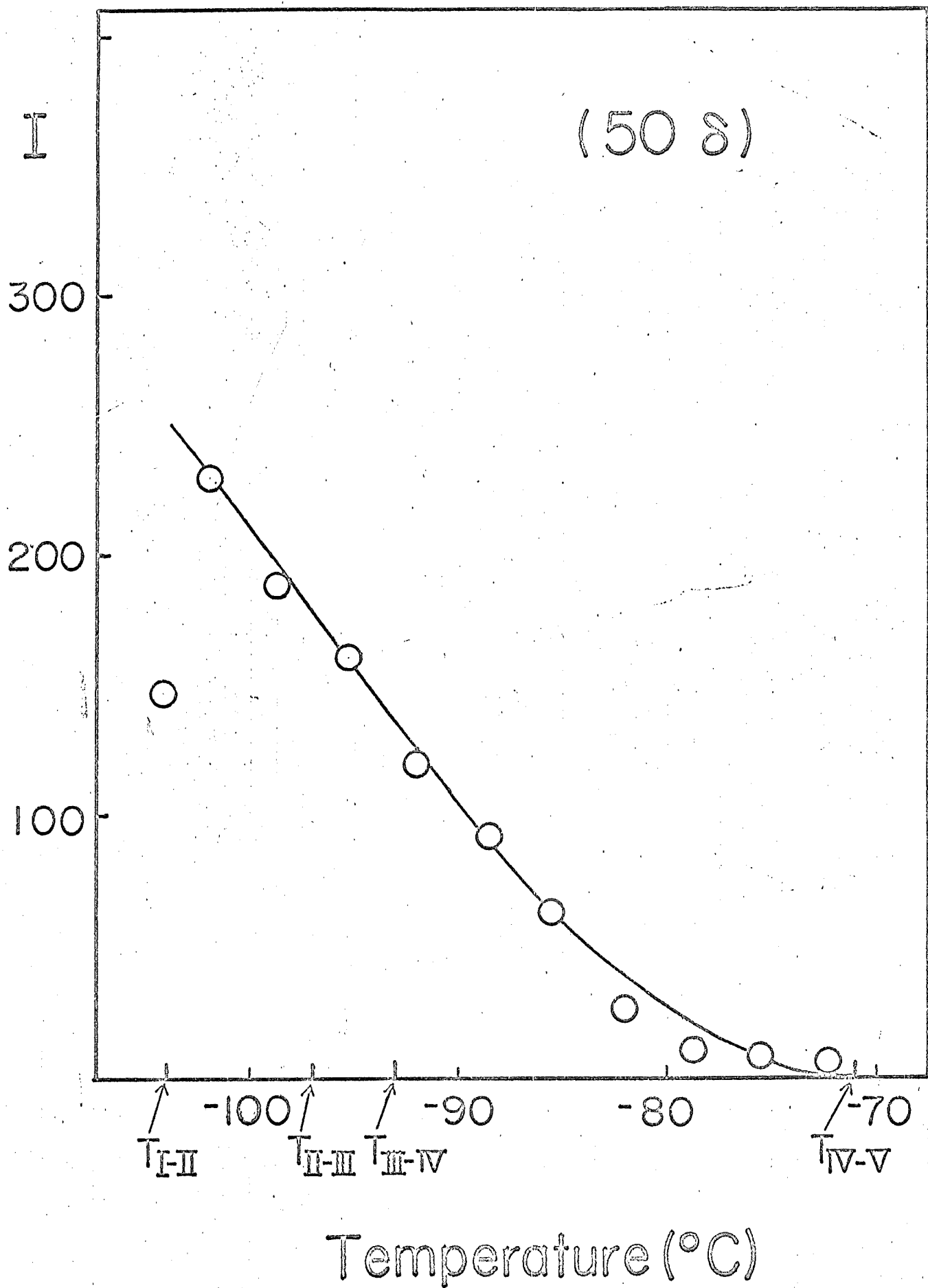


Fig. 10.

ω

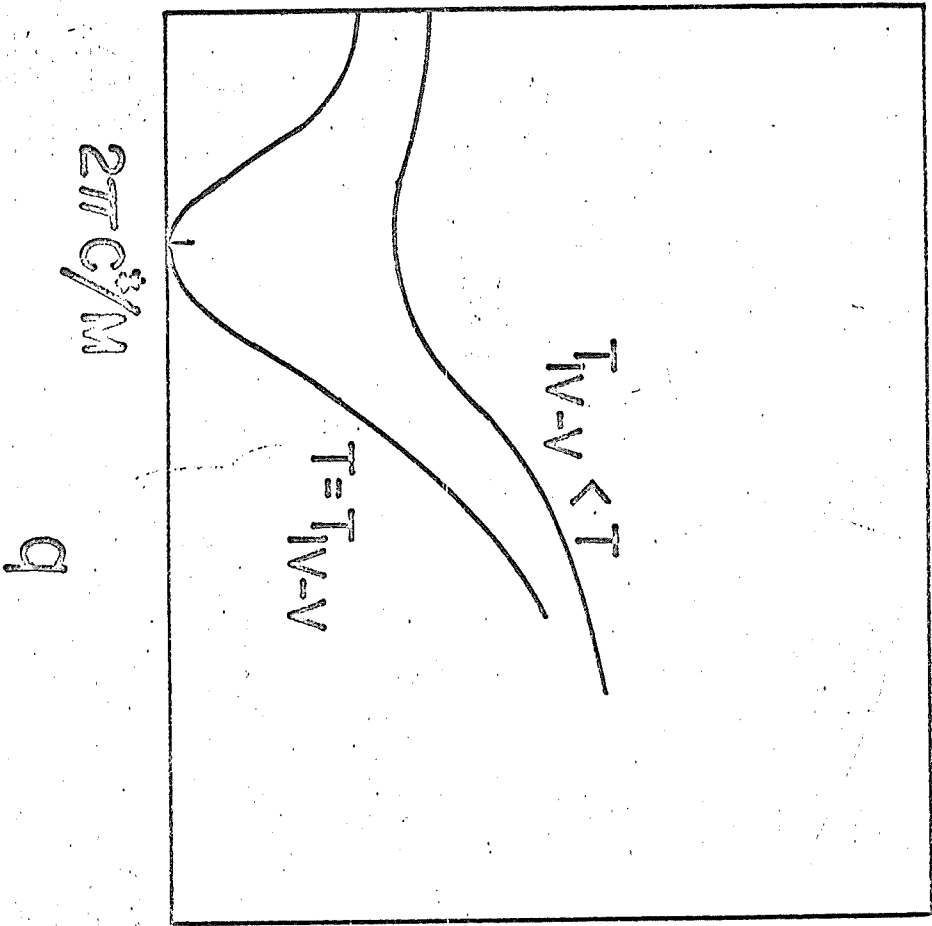


Fig. 11.